Research Article | Vol. 25, No. 17 | 21 Aug 2017 | OPTICS EXPRESS 20437
Optics EXPRESS

Full stabilization and characterization of an optical frequency comb from a diode-pumped solid-state laser with GHz repetition rate

SARGIS HAKOBYAN,[1,*] VALENTIN J. WITTWER,[1] PIERRE BROCHARD,[1] KUTAN GÜREL,[1] STÉPHANE SCHILT,[1] ALINE S. MAYER,[2] URSULA KELLER,[2] AND THOMAS SÜDMEYER[1]

[1]*Laboratoire Temps-Fréquence, Université de Neuchâtel, CH-2000 Neuchâtel, Switzerland*
[2]*Department of Physics, Institute of Quantum Electronics, ETH Zurich, CH-8093 Zürich, Switzerland*
**sargis.hakobyan@unine.ch*

Abstract: We demonstrate the first self-referenced full stabilization of a diode-pumped solid-state laser (DPSSL) frequency comb with a GHz repetition rate. The Yb:CALGO DPSSL delivers an average output power of up to 2.1 W with a typical pulse duration of 96 fs and a center wavelength of 1055 nm. A carrier-envelope offset (CEO) beat with a signal-to-noise ratio of 40 dB (in 10-kHz resolution bandwidth) is detected after supercontinuum generation and *f*-to-2*f* interferometry directly from the output of the oscillator, without any external amplification or pulse compression. The repetition rate is stabilized to a reference synthesizer with a residual integrated timing jitter of 249 fs [10 Hz – 1 MHz] and a relative frequency stability of 10^{-12}/s. The CEO frequency is phase-locked to an external reference via pump current feedback using home-built modulation electronics. It achieves a loop bandwidth of ~150 kHz, which results in a tight CEO lock with a residual integrated phase noise of 680 mrad [1 Hz – 1 MHz]. We present a detailed characterization of the GHz frequency comb that combines a noise analysis of the repetition rate f_{rep}, of the CEO frequency f_{CEO}, and of an optical comb line at 1030 nm obtained from a virtual beat with a narrow-linewidth laser at 1557 nm using a transfer oscillator. An optical comb linewidth of about 800 kHz is assessed at 1-s observation time, for which the dominant noise sources of f_{rep} and f_{CEO} are identified.

OCIS codes: (140.4050) Mode-locked lasers; (140.3425) Laser stabilization; (120.3940) Metrology.

References and links

1. H. R. Telle, G. Steinmeyer, A. E. Dunlop, J. Stenger, D. H. Sutter, and U. Keller, "Carrier-envelope offset phase control: A novel concept for absolute optical frequency measurement and ultrashort pulse generation," Appl. Phys. B **69**(4), 327–332 (1999).
2. D. J. Jones, S. A. Diddams, J. K. Ranka, A. Stentz, R. S. Windeler, J. L. Hall, and S. T. Cundiff, "Carrier-envelope phase control of femtosecond mode-locked lasers and direct optical frequency synthesis," Science **288**(5466), 635–640 (2000).
3. A. Apolonski, A. Poppe, G. Tempea, C. Spielmann, T. Udem, R. Holzwarth, T. W. Hänsch, and F. Krausz, "Controlling the phase evolution of few-cycle light pulses," Phys. Rev. Lett. **85**(4), 740–743 (2000).
4. T. W. Hänsch, "Nobel Lecture: Passion for precision," Rev. Mod. Phys. **78**(4), 1297–1309 (2006).
5. J. Ye, H. Schnatz, and L. W. Hollberg, "Optical frequency combs: From frequency metrology to optical phase control," IEEE J. Sel. Top. Quantum Electron. **9**(4), 1041–1058 (2003).
6. S. A. Diddams, L. Hollberg, and V. Mbele, "Molecular fingerprinting with the resolved modes of a femtosecond laser frequency comb," Nature **445**(7128), 627–630 (2007).
7. S. Schiller, "Spectrometry with frequency combs," Opt. Lett. **27**(9), 766–768 (2002).
8. S. A. Diddams, T. Udem, J. C. Bergquist, E. A. Curtis, R. E. Drullinger, L. Hollberg, W. M. Itano, W. D. Lee, C. W. Oates, K. R. Vogel, and D. J. Wineland, "An optical clock based on a single trapped $^{199}Hg^{+}$ ion," Science **293**(5531), 825–828 (2001).
9. U. Sterr, C. Degenhardt, H. Stoehr, C. Lisdat, H. Schnatz, J. Helmcke, F. Riehle, G. Wilpers, C. Oates, and L. Hollberg, "The optical calcium frequency standards of PTB and NIST," C. R. Phys. **5**(8), 845–855 (2004).
10. C.-H. Li, A. J. Benedick, P. Fendel, A. G. Glenday, F. X. Kärtner, D. F. Phillips, D. Sasselov, A. Szentgyorgyi, and R. L. Walsworth, "A laser frequency comb that enables radial velocity measurements with a precision of 1 cm s^{-1}," Nature **452**(7187), 610–612 (2008).

#294591 https://doi.org/10.1364/OE.25.020437
Journal © 2017 Received 28 Apr 2017; revised 6 Jul 2017; accepted 19 Jul 2017; published 14 Aug 2017

Optics EXPRESS

11. T. Steinmetz, T. Wilken, C. Araujo-Hauck, R. Holzwarth, T. W. Hänsch, L. Pasquini, A. Manescau, S. D'Odorico, M. T. Murphy, T. Kentischer, W. Schmidt, and T. Udem, "Laser frequency combs for astronomical observations," Science **321**(5894), 1335–1337 (2008).
12. T. M. Fortier, M. S. Kirchner, F. Quinlan, J. Taylor, J. C. Bergquist, T. Rosenband, N. Lemke, A. Ludlow, Y. Jiang, C. W. Oates, and S. A. Diddams, "Generation of ultrastable microwaves via optical frequency division," Nat. Photonics **5**(7), 425–429 (2011).
13. X. Xie, R. Bouchand, D. Nicolodi, M. Giunta, W. Hänsel, M. Lezius, A. Joshi, S. Datta, C. Alexandre, M. Lours, P.-A. Tremblin, G. Santarelli, R. Holzwarth, and Y. Le Coq, "Photonic microwave signals with zeptosecond-level absolute timing noise," Nat. Photonics **11**(1), 44–47 (2017).
14. A. Bartels, D. Heinecke, and S. A. Diddams, "10-GHz self-referenced optical frequency comb," Science **326**(5953), 681 (2009).
15. J. Rauschenberger, T. Fortier, D. Jones, J. Ye, and S. Cundiff, "Control of the frequency comb from a modelocked Erbium-doped fiber laser," Opt. Express **10**(24), 1404–1410 (2002).
16. N. R. Newbury and W. C. Swann, "Low-noise fiber-laser frequency combs," J. Opt. Soc. Am. B **24**(8), 1756–1770 (2007).
17. D. C. Heinecke, A. Bartels, and S. A. Diddams, "Offset frequency dynamics and phase noise properties of a self-referenced 10 GHz Ti:sapphire frequency comb," Opt. Express **19**(19), 18440–18451 (2011).
18. S. Schilt and T. Südmeyer, "Carrier-Envelope Offset Stabilized Ultrafast Diode-Pumped Solid-State Lasers," Appl. Sci. **5**(4), 787–816 (2015).
19. K. Gürel, V. J. Wittwer, S. Hakobyan, S. Schilt, and T. Südmeyer, "Carrier envelope offset frequency detection and stabilization of a diode-pumped mode-locked Ti:sapphire laser," Opt. Lett. **42**(6), 1035–1038 (2017).
20. M. Endo, I. Ito, and Y. Kobayashi, "Direct 15-GHz mode-spacing optical frequency comb with a Kerr-lens mode-locked Yb:$Y_{(2)}O_{(3)}$ ceramic laser," Opt. Express **23**(2), 1276–1282 (2015).
21. A. Klenner, M. Golling, and U. Keller, "A gigahertz multimode-diode-pumped Yb:KGW enables a strong frequency comb offset beat signal," Opt. Express **21**(8), 10351–10357 (2013).
22. S. A. Meyer, T. M. Fortier, S. Lecomte, and S. A. Diddams, "A frequency-stabilized Yb:KYW femtosecond laser frequency comb and its application to low-phase-noise microwave generation," Appl. Phys. B **112**(4), 565–570 (2013).
23. A. Klenner, S. Schilt, T. Südmeyer, and U. Keller, "Gigahertz frequency comb from a diode-pumped solid-state laser," Opt. Express **22**(25), 31008–31019 (2014).
24. A. Klenner, A. S. Mayer, A. R. Johnson, K. Luke, M. R. E. Lamont, Y. Okawachi, M. Lipson, A. L. Gaeta, and U. Keller, "Gigahertz frequency comb offset stabilization based on supercontinuum generation in silicon nitride waveguides," Opt. Express **24**(10), 11043–11053 (2016).
25. A. S. Mayer, A. Klenner, A. Johnson, K. Luke, M. Lamont, Y. Okawachi, M. Lipson, A. Gaeta, and U. Keller, "Low-noise Gigahertz Frequency Comb from diode-Pumped Solid-State Laser using Silicon Nitride Waveguides," in *Advanced Solid State Lasers* (Optical Society of America, 2015), paper ATh4A–5.
26. S. A. Meyer, J. A. Squier, and S. A. Diddams, "Diode-pumped Yb:KYW femtosecond laser frequency comb with stabilized carrier-envelope offset frequency," Eur. Phys. J. D **48**(1), 19–26 (2008).
27. M. C. Stumpf, S. Pekarek, A. E. H. Oehler, T. Südmeyer, J. M. Dudley, and U. Keller, "Self-referencable frequency comb from a 170-fs, 1.5-µm solid-state laser oscillator," Appl. Phys. B **99**(3), 401–408 (2010).
28. S. Schilt, N. Bucalovic, V. Dolgovskiy, C. Schori, M. C. Stumpf, G. Di Domenico, S. Pekarek, A. E. H. Oehler, T. Südmeyer, U. Keller, and P. Thomann, "Fully stabilized optical frequency comb with sub-radian CEO phase noise from a SESAM-modelocked 1.5-µm solid-state laser," Opt. Express **19**(24), 24171–24181 (2011).
29. N. Torcheboeuf, G. Buchs, S. Kundermann, E. Portuondo-Campa, J. Bennès, and S. Lecomte, "Repetition rate stabilization of an optical frequency comb based on solid-state laser technology with an intra-cavity electro-optic modulator," Opt. Express **25**(3), 2215–2220 (2017).
30. C.-C. Lee, Y. Hayashi, D. Hou, K. Silverman, A. Feldman, T. Harvey, R. Mirin, and T. R. Schibli, "Highly phase-coherent stabilization of carrier-envelope-offset frequency with graphene modulator on SESAM," in *Conference on Lasers and Electro-Optics (2016)* (Optical Society of America, 2016), paper SM3H.7.
31. T. D. Shoji, W. Xie, K. L. Silverman, A. Feldman, T. Harvey, R. P. Mirin, and T. R. Schibli, "Ultra-low-noise monolithic mode-locked solid-state laser," Optica **3**(9), 995–998 (2016).
32. S. Schilt, N. Bucalovic, L. Tombez, V. Dolgovskiy, C. Schori, G. Di Domenico, M. Zaffalon, and P. Thomann, "Frequency discriminators for the characterization of narrow-spectrum heterodyne beat signals: application to the measurement of a sub-hertz carrier-envelope-offset beat in an optical frequency comb," Rev. Sci. Instrum. **82**(12), 123116 (2011).
33. A. Schlatter, S. C. Zeller, R. Grange, R. Paschotta, and U. Keller, "Pulse-energy dynamics of passively mode-locked solid-state lasers above the *Q*-switching threshold," J. Opt. Soc. Am. B **21**(8), 1469–1478 (2004).
34. F. Emaury, A. Diebold, A. Klenner, C. J. Saraceno, S. Schilt, T. Südmeyer, and U. Keller, "Frequency comb offset dynamics of SESAM modelocked thin disk lasers," Opt. Express **23**(17), 21836–21856 (2015).
35. G. Di Domenico, S. Schilt, and P. Thomann, "Simple approach to the relation between laser frequency noise and laser line shape," Appl. Opt. **49**(25), 4801–4807 (2010).
36. V. Dolgovskiy, N. Bucalovic, P. Thomann, C. Schori, G. Di Domenico, and S. Schilt, "Cross-influence between the two servo loops of a fully stabilized Er: fiber optical frequency comb," J. Opt. Soc. Am. B **29**(10), 2944–2957 (2012).

Optics EXPRESS

37. D. A. Howe, D. U. Allan, and J. A. Barnes, "Properties of Signal Sources and Measurement Methods," in *Proceedings of the 35th Annual Frequency Control Symposium* (IEEE, 1981), pp. 669–716.
38. M. Beck, A. Cox, T. Plötzing, M. Indlekofer, T. Mandhyani, P. Leiprecht, and A. Bartels, "Turn-key 1 GHz Ti:sapphire frequency comb with enhanced offset locking bandwidth," in *8th Frequency Standard and Metrology Symposium* (2015), poster D04.
39. M. Hoffmann, S. Schilt, and T. Südmeyer, "CEO stabilization of a femtosecond laser using a SESAM as fast opto-optical modulator," Opt. Express **21**(24), 30054–30064 (2013).
40. S. Hakobyan, V. J. Wittwer, K. Gürel, P. Brochard, S. Schilt, A. S. Mayer, U. Keller, and T. Südmeyer, "Opto-Optical Modulator for CEO Control and Stabilization in an Yb:CALGO GHz Diode-Pumped Solid-State Laser," in *The European Conference on Lasers and Electro-Optics* (Optical Society of America, 2017), paper CF-1.1.
41. H. R. Telle, B. Lipphardt, and J. Stenger, ""Kerr-lens, mode-locked lasers as transfer oscillators for optical frequency measurements," Appl. Phys," B Lasers Opt. **74**(1), 1–6 (2002).

1. Introduction

Fully-stabilized optical frequency combs from modelocked lasers have revolutionized many fields in optics and physics by enabling ultra-precise measurements and by providing a direct and coherent link between the optical and microwave spectral domains [1–3]. Frequency combs constitute today a key component in various applications ranging from optical frequency metrology [4,5] to ultra-high resolution broadband spectroscopy [6,7] and optical atomic clocks [8,9] that have become the most stable clocks existing today. Some of these applications, such as the calibration of astronomical spectrographs [10,11] or the generation of ultra-low-noise microwave signals [12,13] can benefit from frequency combs with a high repetition rate, which provide a higher optical power per comb mode for a given average power and facilitate the spectral filtering of individual modes.

So far, modelocked frequency combs with GHz repetition rates have been demonstrated essentially from ultrafast Ti:Sapphire lasers, reaching up to a record-high repetition rate of 10 GHz for a self-referenced comb [14]. The most established comb technology today is based on modelocked fiber lasers [15,16]. However, they are not well suited for high repetition rate operation due to the conjunction of high optical losses and limited gain per unit length of fiber cavities. Furthermore, fiber lasers generally suffer from a higher noise level than their solid-state resonator counterparts, which notably results from their lower Q-factor. This makes the stabilization of the carrier-envelope offset (CEO) frequency in high repetition rate fiber lasers challenging, since the CEO noise typically scales with the repetition rate [17]. Modelocked diode-pumped solid-state lasers (DPSSL) [18] are an excellent technology for GHz frequency combs, as they combine the advantages of simple diode pumping schemes with low loss optical resonators leading to suitable noise properties for comb stabilization. DPSSL combs can operate with various gain materials operating in different wavelength regions, for example Ti:Sapphire [19] around 780 nm, Ytterbium (Yb) doped materials around 1 µm [20–26] and Erbium (Er) around 1.5 µm [27–30]. Self-referenced frequency combs from modelocked DPSSLs with a repetition rate in the GHz regime have been demonstrated from a few platforms like Yb:CALGO DPSSLs [23–25] or from a monolithic extremely low-noise Er:Yb:glass solid-state laser [31]. However, only the CEO frequency f_{CEO} was stabilized in these cases, and the second degree of freedom of the comb, i.e., the repetition rate frequency f_{rep}, was left free-running. On the other hand, a 15-GHz Yb:Y_2O_3 ceramic DPSSL was fully-stabilized by means of repetition rate locking on one side, and stabilization of one comb line to an ultra-stable laser using a feedforward stabilization on the other side [20]. However, this comb was not self-referenced and suffers from the frequency drift of the reference laser in comparison to a CEO-stabilized comb.

Detecting and stabilizing the CEO frequency represents a major challenge for lasers in the GHz regime and has often been the center of interest in past publications. Full control of the comb, however, can only be achieved with additional repetition rate stabilization and the careful design of each feedback loop to avoid cross-talks is non-trivial. In addition, understanding the influence of both repetition rate and CEO control on the properties of

Optics EXPRESS

individual optical comb lines is especially relevant for applications such as comb spectroscopy, where the noise and linewidth of the actual optical combs line matter.

In this work, we demonstrate the first self-referenced full stabilization of a frequency comb from a modelocked DPSSL in the 1-µm spectral range with a GHz repetition rate. The Yb:CALGO laser was phase-stabilized by feedback to the cavity length using a piezoelectric transducer (PZT) for f_{rep} and to the pump diode current for f_{CEO} [15]. We present a thorough noise analysis of the resulting frequency comb by individually characterizing the noise properties of f_{rep}, f_{CEO} and of an optical comb line obtained from the heterodyne beat with a narrow-linewidth continuous-wave laser. Finally, we show that the intensity noise of the pump diode and mechanical noise induced by its water cooling constitute the main contributions to the CEO phase noise.

2. Yb:CALGO GHz DPSSL

The modelocked laser is based on a previously reported design [23]. It consists of a 2-mm thick Yb:CALGO crystal with an asymmetric cut (a-cut) to prevent multi-polarization operation. The crystal, doped with 5% of Yb, is pumped by a commercial diode laser array (LIMO F100-DL980-EX1930) that can deliver an output power up to 60 W at a central wavelength of 980 nm out of a highly multimode fiber (core diameter of 100 µm, NA of 0.22). The emission wavelength of the pump diode is stabilized by a volume holographic grating (VHG), resulting in lower relative intensity noise (RIN) of the diode and thus lower amplitude noise of the modelocked laser [24]. The pump diode is unpolarized, hence a polarizing beamsplitter (PBS) is used to select the s-polarization to pump the crystal (see the experimental scheme depicted in Fig. 1), resulting in only one half of the diode power effectively used to pump the laser. The cavity has a length of 14.2 cm, corresponding to a repetition rate of 1.05 GHz.

The cavity consists of a dichroic end mirror (M1) that is transmissive at the pump wavelength and highly reflective at the lasing wavelength. It is followed by a curved dispersive mirror (M2) with a radius of curvature of 75 mm, which provides a negative dispersion of –400 fs^2 per bounce. This mirror has a high transmission at the pump wavelength to remove residual pump light. An output coupler (OC) with 1% transmission is used as a folding mirror, resulting in two distinct output beams. A semiconductor saturable absorber mirror (SESAM) is mounted on a PZT driven by a high-voltage amplifier (HVA) for cavity length control (f_{rep} stabilization) and acts as the second cavity end mirror (see Fig. 1). The SESAM has a modulation depth of 1.15%, nonsaturable loss of 0.07%, and a saturation fluence of 10.69 µJ/cm^2.

Optics EXPRESS

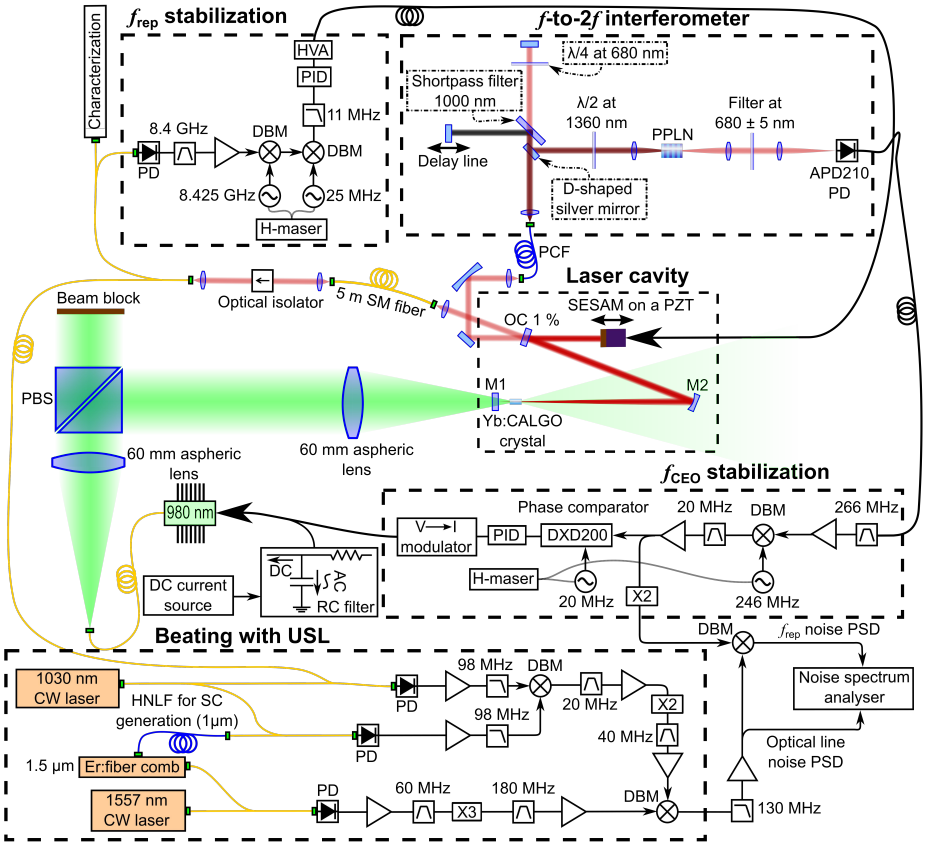

Fig. 1. Overall scheme of the fully-stabilized Yb:CALGO GHz frequency comb and of its noise characterization. The laser cavity (center) is pumped by a 980-nm fiber-coupled diode array (left). One output beam of the laser is launched into a PCF for SC spectrum generation, followed by an *f*-to-2*f* interferometer for CEO detection (top). The stabilization of f_{CEO} is implemented by a phase-lock loop with feedback applied to the pump diode current through a home-built voltage-to-current (V→I) modulator (middle-bottom), whereas f_{rep} is stabilized to an H-maser (through frequency synthesizers) by cavity length control with a PZT (top left). Finally, an optical line of the GHz comb is characterized from its heterodyne beat with an ultra-stable laser (USL) at 1.56 μm using an Er:fiber comb as a transfer oscillator (bottom). PD: photodiode; PPLN: periodically-poled lithium niobate; PCF: photonic-crystal fiber; HNLF: highly nonlinear fiber; PID: proportional-integral-derivative controller; DBM: double-balanced mixer; HVA: high-voltage amplifier. Yellow lines represent singlemode (SM) optical fiber connections, red, pink and green lines schematize free-space optical beams, and black lines are electrical connections.

Optics EXPRESS

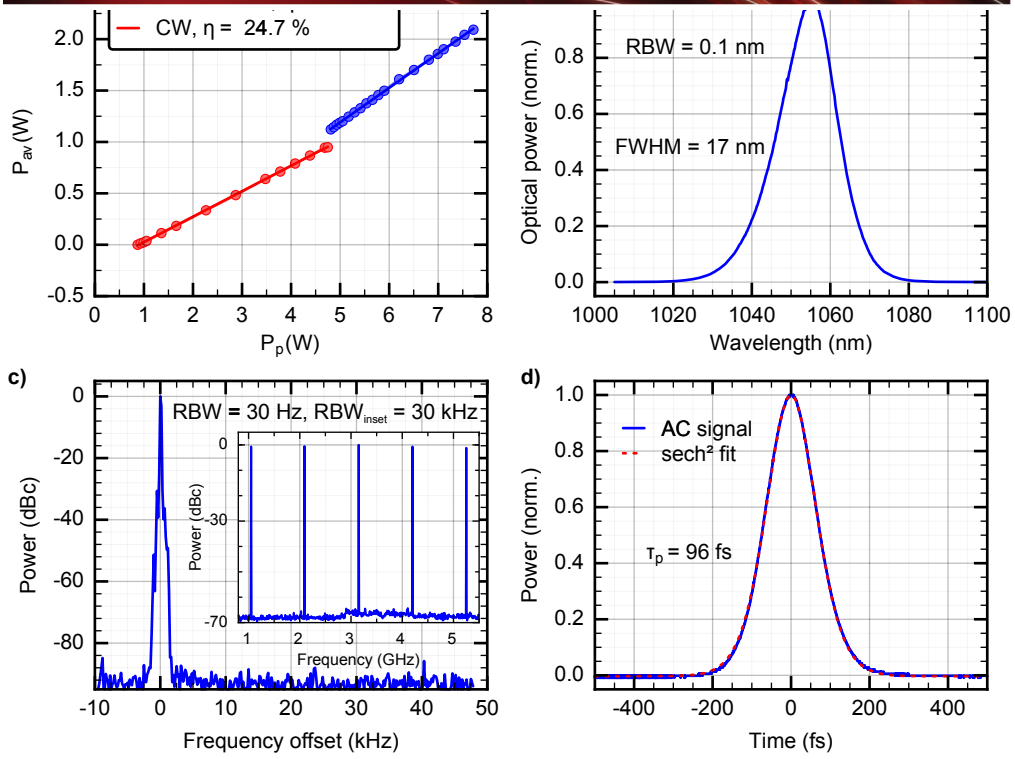

Fig. 2. a) Average output power vs pump power for CW and modelocked (ML) operations; b) Optical spectrum of the laser in ML operation; c) Normalized RF spectrum of the laser in ML operation, offset from the fundamental f_{rep} = 1.05 GHz; inset c) first five harmonics of f_{rep}; d) Autocorrelation (AC) trace of an optical pulse of the laser (blue trace) with a sech^2 fit (dashed red line).

The laser starts emitting in continuous wave (CW) mode at a threshold pump power of 870 mW incident to the dichroic mirror (M1) and has a slope efficiency of 24.7% up to a pump power of ~4.8 W (corresponding to ~1 W of CW output power). Then, self-starting SESAM-modelocked operation occurs for pump powers ranging from ~4.8 W to the maximum used value of 7.7 W [Fig. 2(a)]. The maximum average output power of the laser is 2.1 W in modelocked operation with a slope efficiency of 33.5%. The laser emits an optical spectrum with a full width at half maximum (FWHM) of 17 nm centered at 1055 nm [Fig. 2(b)], in 96-fs pulses [Fig. 2(d)] at a fundamental repetition rate of 1.05 GHz [Fig. 2(c)]. One of the output beams is used for f_{rep} stabilization and comb characterization, whereas the other one is used for supercontinuum (SC) spectrum generation, f_{CEO} detection and stabilization.

3. Carrier-envelope-offset (CEO) detection

One of the two output beams of the laser is sent to a 1-m long photonic crystal fiber (PCF) with a zero dispersion wavelength of 945 nm for SC spectrum generation. The coupling efficiency is ~80%, leading to an effective average power of 670 mW being coupled into the PCF. The SC spectrum measured at the output of the PCF spans over a full frequency octave ranging from ~650 nm to ~1420 nm at –35 dB from the maximum power achieved at ~1350 nm (Fig. 3). This spectrum is then sent into a traditional *f*-to-2*f* interferometer (see Fig. 1) for CEO detection [1]. The SC spectrum is separated at the input of the *f*-to-2*f* interferometer into short and long wavelength components centered at 680 nm and 1360 nm, respectively, using a low-pass optical filter with a cut-off wavelength of ~1000 nm. The two beams propagate in two different optical paths, where they are reflected back by a mirror and are recombined using the same optical filter. An adjustable delay line in the long-wavelength path enables adjusting the temporal overlap of the fundamental and frequency-doubled pulses

Optics EXPRESS

on the photodiode at the output of the interferometer. A D-shaped mirror reflects the long and short wavelength components into a periodically-poled lithium niobate (PPLN) crystal with a poling period of 14.08 μm for second harmonic generation (SHG). A half-wave plate is used in the common path to align the polarization of the 1360-nm beam for efficient SHG. Another waveplate in the 680-nm arm enables adjusting the polarization of this component for optimized CEO beat generation. The PPLN is heated to 50°C for efficient SHG at 1360 nm. The 680-nm light at the output of the PPLN is focused onto a silicon avalanche photodiode for CEO beat detection (see Fig. 1). A CEO beat with a signal-to-noise ratio (SNR) of ~40 dB was detected in a resolution bandwidth (RBW) of 10 kHz (Fig. 4).

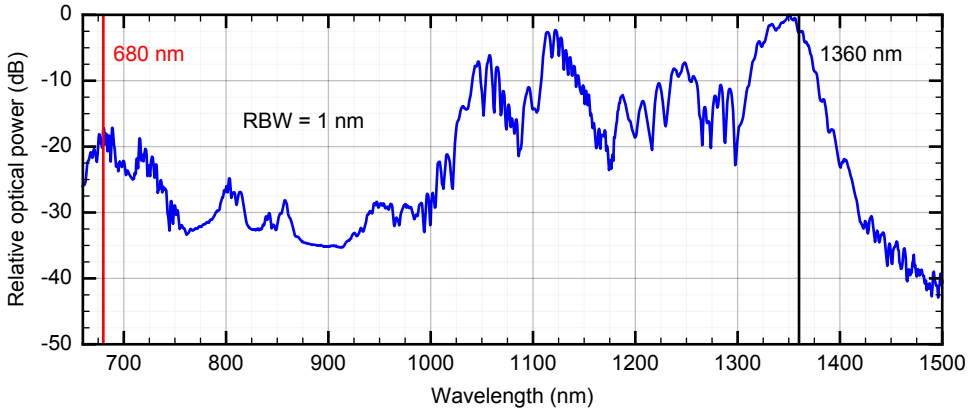

Fig. 3. Full octave-spanning SC spectrum measured at the output of the PCF. The *f* and 2*f* frequency components used for CEO detection in the *f*-to-2*f* interferometer are indicated by the black and red vertical lines, respectively. The spectrum is normalized with respect to the maximum spectral power achieved at 1350 nm; the total power at the output of the PCF is ~670 mW.

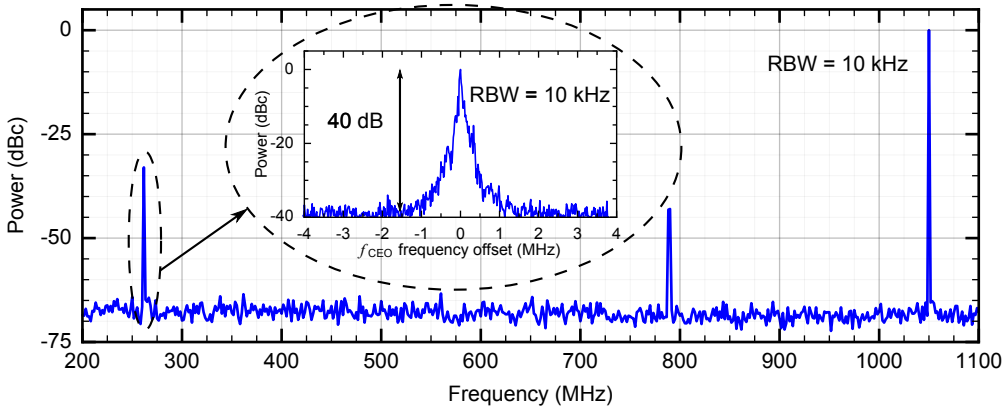

Fig. 4. RF spectrum of the signal at the output of the *f*-to-2*f* interferometer showing a CEO frequency of ~266 MHz. The inset displays a zoom on the CEO beat showing an SNR of 40 dB in a RBW of 10 kHz.

4. Frequency comb full stabilization

4.1 Static and dynamic comb control

Prior to the comb stabilization, we measured the static and dynamic tuning rates of f_{rep} and f_{CEO} as a function of the PZT voltage and pump current, respectively (Fig. 5). Whereas the static measurements aimed at determining the maximum span over which f_{rep} and f_{CEO} can be linearly shifted, the dynamic measurements provide useful information about the frequency-dependent amplitude and phase response of f_{rep} and f_{CEO} upon modulation, which are important parameters to assess the achievable locking bandwidth in a stabilization loop.

Optics EXPRESS

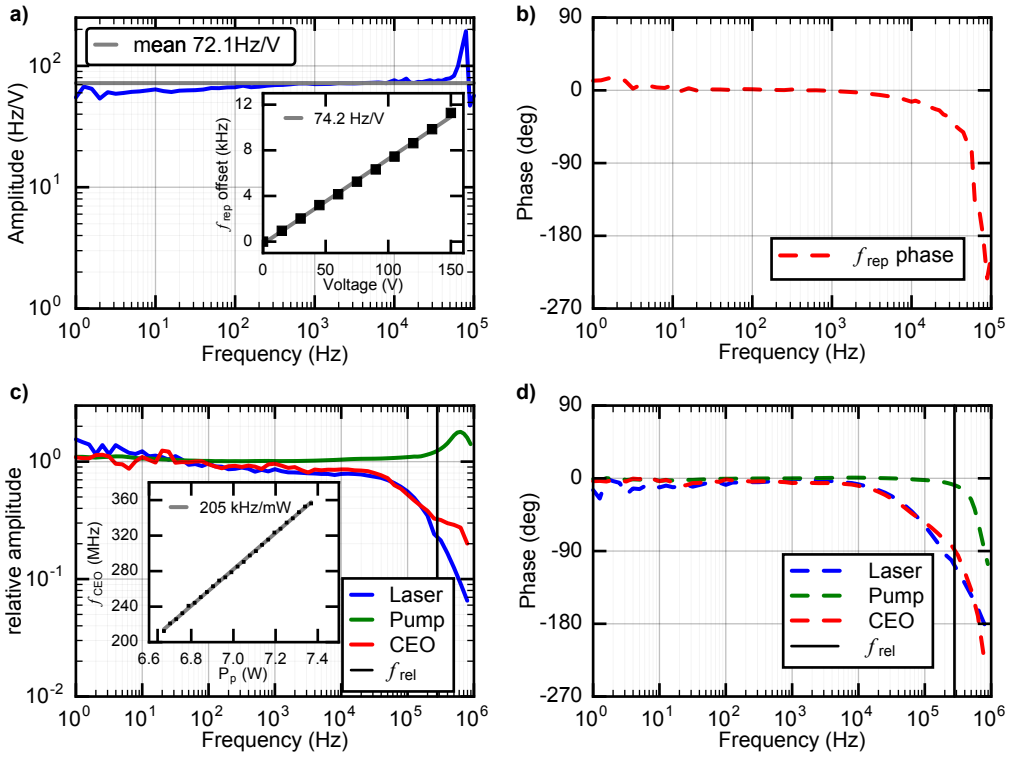

Fig. 5. a) Amplitude of the transfer function of f_{rep} for PZT modulation (blue) and calculated mean value (gray); inset: static tuning of f_{rep} as a function of the PZT voltage. b) Phase of the transfer function of f_{rep} for PZT modulation (dashed red). c) Relative amplitude of the transfer functions of f_{CEO} (red), of the laser output power (blue), and of the pump optical power (green) for pump current modulation, and calculated relaxation frequency (f_{rel}) of the laser (straight black line); inset: static tuning of f_{CEO} as a function of pump current. d) Phase of the transfer functions of f_{CEO} (red), of the laser output power (blue), and of the pump optical power (green) for pump current modulation, and calculated relaxation frequency (f_{rel}) of the laser (straight black line).

The static curves displayed in the insets of Fig. 5(a) and 5(c) show a linear response with a tuning coefficient of 74.2 Hz/V over a span of ~12 kHz for f_{rep} as a function of the voltage at the output of the HVA, and 205 kHz/mW over a span of ~150 MHz for f_{CEO} as a function of the pump power, respectively. These tuning ranges are limited by the 150-V driving voltage of the PZT for f_{rep}, and by the range of detectable CEO beat for f_{CEO}. However, both tuning ranges are largely sufficient for precise adjustment and stabilization of these frequencies.

For the dynamic curves, we modulated either the voltage at the input of the HVA or in our home-made pump current source with a sine waveform, corresponding typically to a modulation of 80 V applied to the PZT or of 150 mW of the pump power. The resulting frequency modulation was measured in amplitude and phase by demodulating the repetition rate or CEO beat using a frequency discriminator [32], followed by a lock-in amplifier (HFLI2 from Zurich Instrument) set to the applied modulation frequency. The measured transfer function of f_{rep} displayed in Fig. 5(a) shows a flat response in amplitude up to more than 50 kHz, followed by a narrow resonance peak at ~80 kHz. The amplitude of the transfer function of ~72.1 Hz/V observed at low modulation frequency is in excellent agreement with the aforementioned static value that was separately measured using an RF spectrum analyzer. The phase of the transfer function remains close to zero for frequencies up to 10 kHz and a phase shift of 90° is reached at ~60 kHz [Fig. 5(b)]. For f_{CEO}, the measured transfer function behaves like a low-pass filter with a 3-dB cut-off frequency of ~100 kHz and a 90° phase

Optics EXPRESS

shift reached at a modulation frequency of ~280 kHz [Fig. 5(d)]. For comparison, the transfer function of the output power of the pump diode modulated by our home-made driver was also measured by detecting a small fraction of the pump power on a photodiode and performing similar lock-in detection. The achieved modulation bandwidth of the pump power was larger than 1 MHz in amplitude (with the presence of a small overshoot at ~700 kHz). Therefore, the observed modulation bandwidth of f_{CEO} in our modelocked laser is not limited by the pump response, but by the relaxation oscillation that accounts in particular for the upper state lifetime of the gain medium and the cavity dynamics. We calculated a relaxation oscillation of ~280 kHz for our laser [33] [straight black lines in Fig. 5(c)–5(d)], which is in good agreement with the 90° phase shift of the CEO transfer function observed at ~280 kHz. For cross-check, we also measured the transfer function of the output power of the modelocked laser, which is influenced by the same dynamics and usually shows a very similar behavior as f_{CEO} [34], which is indeed the case in the present modelocked laser as shown in Fig. 5(c)–5(d).

4.2 Stabilization schemes

The stabilization schemes implemented to phase-lock f_{rep} and f_{CEO} to reference frequencies are depicted in the correspondingly labeled frames in Fig. 1.

For repetition rate stabilization, the 8th harmonic of f_{rep} at ~8.4 GHz was chosen to enhance the phase noise sensitivity compared to the fundamental component. It was detected using a high-bandwidth photodiode (New Focus 1434) with a small fraction of one of the laser output beams. The signal was filtered, amplified and frequency down-converted to ~25 MHz by mixing it with the signal of a reference synthesizer (Rohde-Schwarz SMF-100A). The down-converted signal was compared in a second double-balanced mixer (DBM) to the reference signal from a second signal synthesizer (SRS DS345). To ensure stable long-term operation of the comb, both synthesizers were referenced to an H-maser. The resulting phase error signal was low-pass filtered and processed by a servo-controller to produce the correction signal to control the cavity length of the laser. This signal was amplified by a high-voltage amplifier (gain of 15) and applied to the PZT holding the SESAM in the cavity.

For f_{CEO} stabilization, the CEO beat detected at the output of the *f*-to-2*f* interferometer at ~266 MHz was low-pass filtered, amplified and frequency down-converted to ~20 MHz using a synthesizer and a DBM. The down-converted CEO beat signal was band-pass filtered, amplified to ~0 dBm and compared in a digital phase detector (DXD200 from Menlo Systems) to a ~20-MHz reference signal. All frequency references were locked to the same H-maser as used for f_{rep} stabilization. The phase error signal was processed by a proportional-integral-derivative (PID) controller (Vescent D2-125) and the resulting feedback signal was applied to the current of the pump diode. To achieve the fast pump modulation that is required for CEO stabilization, we developed a home-made voltage-to-current converter with a modulation bandwidth of ~1 MHz and a gain of 120 mA/V, which was used to drive the pump diode in parallel with a high current source (Delta Elektronika SM 18-50) delivering the typical bias current of 17.7 A for the diode. A low-pass RC filter with a nominal cut-off frequency of ~16 Hz was placed between the current source and the pump diode for a double purpose. First, it reduced the current noise of the DC source coupled to the diode, thus decreasing its RIN, especially by strongly filtering out some strong spurious noise peaks occurring at 50 Hz and other discrete frequencies (see Fig. 6). Secondly, it ensured that the modulation signal from the fast current modulator was properly applied to the pump diode, avoiding any cross-coupling to the DC source.

Optics EXPRESS

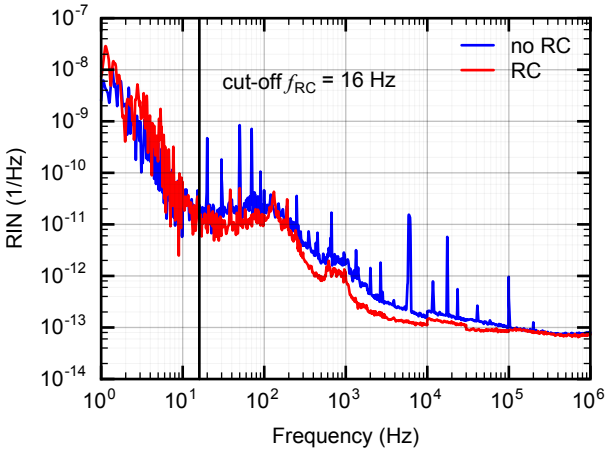

Fig. 6. Comparison of the RIN of the pump diode measured without (blue) and with (red) the RC filter placed between the high current source and the pump diode. The cut-off frequency of the RC filter is indicated by the straight vertical line. The RC filter efficiently suppresses the discrete noise peaks of electrical origin located between 10 and 100 Hz, and in the range of 1 kHz to 100 kHz. The broadband excess noise present at $f > 10$ Hz is not affected by the filter as it arises from a different origin that is discussed in detail in Section 5.2.

5. Characterization of the fully stabilized comb

5.1 Frequency noise of the phase-locked comb parameters

We have characterized the noise properties of the GHz comb, both in free-running and fully-stabilized conditions, by measuring the frequency noise power spectral density (FN-PSD) of the repetition rate and CEO beat using a phase noise analyzer (Rohde & Schwarz FSWP26).

In a first step, we aimed at optimizing the CEO stabilization loop to minimize its residual integrated phase noise. Figure 7(a) shows the measured FN-PSD for the free-running and locked CEO beats. A locking bandwidth of ~150 kHz assessed from the position of the servo bump in the FN-PSD was achieved using our home-made diode current modulator. The FN-PSD of the CEO beat was entirely reduced below the β-separation line [35], indicating the achievement of a tight lock that is characterized by the presence of a coherent peak in the CEO RF spectrum. The observed coherent peak is shown in the inset of Fig. 7(a), with an SNR of 50 dB in a resolution bandwidth of 1 Hz. The integrated phase noise of the stabilized CEO beat was 680 mrad [1 Hz – 1 MHz]. In this first configuration, the stabilization loop for f_{rep} was implemented only with a PI (proportional-integral) servo-controller (Newport LB1005). The resulting FN-PSD of f_{rep} is shown in Fig. 7(b), together with the noise spectrum of the free-running repetition rate. With this stabilization loop, the noise of f_{rep} was reduced to the level of the reference synthesizer at Fourier frequencies up to ~100 Hz. The integrated timing jitter was 519 fs in this case (integrated from 10 Hz to 1 MHz). We found that the noise peaks occurring in the FN-PSD of f_{rep} in the range of ~100 Hz to ~2 kHz [Fig. 7(b)] were originating from mechanical noise. To damp these peaks, we isolated the laser breadboard from the optical table by using damping foam rubber, and we also isolated the water tubes of the pump diode cooling circuit that could transfer some mechanical noise to the optical table. With these changes, the noise peaks at ~100 Hz and ~600 Hz in the FN-PSD of f_{rep} were reduced by approximately one order of magnitude, while the peak at 1 kHz was reduced by nearly two orders of magnitude [compare the blue curves in Fig. 7(b) and Fig. 8(b)].

Optics EXPRESS

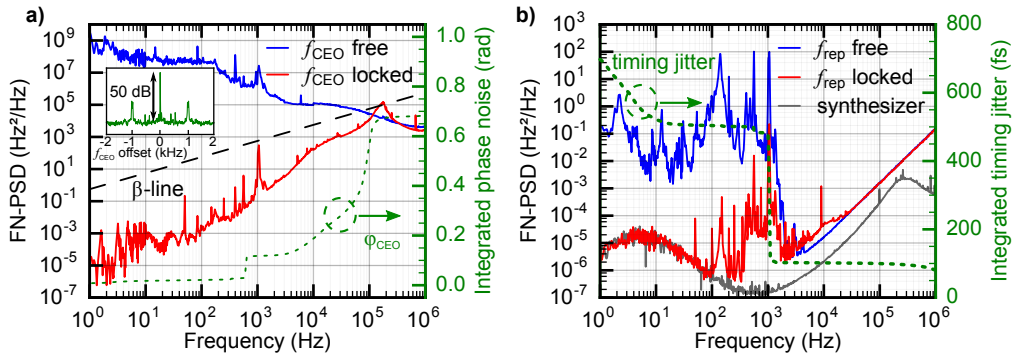

Fig. 7. Noise performance of the fully-stabilized GHz comb obtained using a PID controller for the CEO feedback loop and a PI controller for the repetition rate. a) Frequency noise power spectral density (FN-PSD) of the CEO beat in free-running (blue) and stabilized (red) conditions, and corresponding integrated phase noise as a function of the upper cut-off frequency (right vertical axis); inset: RF spectrum of the CEO beat showing a coherent peak with an SNR of 50 dB at a RBW of 1 Hz. b) FN-PSD of the free-running (blue) and phase-locked (red) repetition rate stabilized using a PI servo gain. The FN-PSD of the reference synthesizer is also shown for comparison (gray). Right vertical axis: integrated timing jitter as a function of the lower cut-off frequency.

To be able to extend the stabilization bandwidth of f_{rep} and further reduce its noise, we used a different servo controller (Vescent D2-125) providing a derivative filter, as well as a second integrator, in addition to the PI gain previously used. With this, the detrimental noise peaks occurring in the FN-PSD of the repetition rate in the frequency range of 100 Hz to 1 kHz have been reduced as shown in Fig. 8(b), leading to an improved timing jitter of 249 fs [10 Hz – 1 MHz]. However, this increased stabilization bandwidth for f_{rep} produced a negative side effect by increasing the noise of the free-running CEO beat as a result of a possible cross-effect of the PZT modulation to the CEO frequency as observed in a fiber comb [36]. As a result, the noise of the stabilized CEO slightly increased around the servo-bump, clearly exceeding the β-separation line. The corresponding integrated phase noise increased to 1.34 rad.

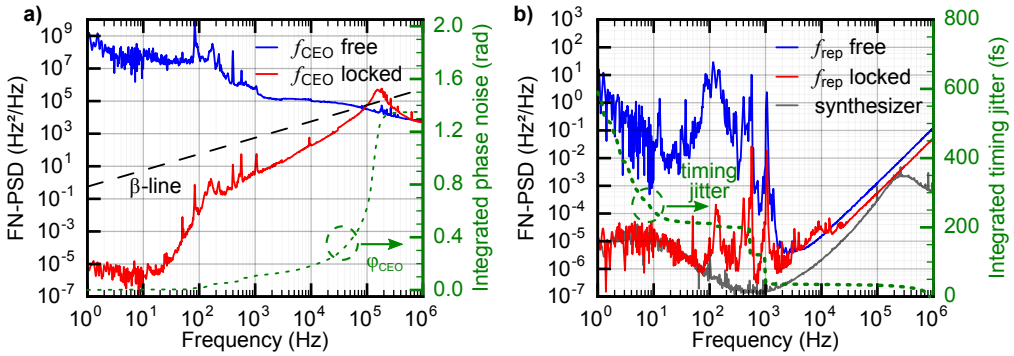

Fig. 8. Noise performance of the fully-stabilized GHz comb obtained with the same CEO feedback loop as in Fig. 7, but with mechanical damping of the laser breadboard and a derivative filter added to the repetition rate feedback loop. a) FN-PSD of the CEO beat in free-running (blue) and stabilized (red) conditions, and corresponding integrated phase noise as a function of the upper cut-off frequency (right vertical axis). b) FN-PSD of the free-running (blue) and phase-locked (red) repetition rate stabilized using a PID servo controller. The FN-PSD of the reference synthesizer is also shown for comparison (gray). Right vertical axis: integrated timing jitter as a function of the lower cut-off frequency.

Optics EXPRESS

5.2 CEO noise source analysis

A further analysis was performed to investigate the dominant noise sources of the CEO beat. First, the RIN of the pump diode was measured and its contribution to the CEO FN-PSD was calculated using the measured transfer function of f_{CEO} for pump current modulation. Figure 9(a) shows an excellent overlap between the contribution of the pump RIN to the CEO noise and the actual CEO noise. This demonstrates that the pump RIN is essentially responsible for the CEO noise, except for some narrow noise peaks that are likely of mechanical origin in the laser cavity. To further investigate the origin of the pump RIN, we also measured the current noise of the DC source used to drive the diode, and converted it into an equivalent CEO frequency noise. This was realized by taking into account the drive-current-to-output-power response of the pump diode and the pump-power-to-CEO-frequency transfer function of the modelocked laser. One can observe in Fig. 9(a) that the current noise of the pump diode driver is responsible for the CEO frequency noise at low Fourier frequencies (< 10 Hz). However, another source of excess noise is dominant at higher frequencies.

To identify the origin of this excess noise, we measured the RIN of the pump diode with its water cooling circuit switched on and off. A significant difference in the pump RIN was observed in these two cases as displayed in Fig. 9(b). The RIN of the pump diode is larger at low Fourier frequencies without the water cooling due to a thermal drift resulting in a linear shift of its optical output power. However, the noise is significantly larger at higher frequencies when the water cooling is activated, and the RIN presents the same noise pattern as the CEO beat. Therefore, the water cooling circuit has a strong contribution to the excess RIN of the pump diode. The fact that the water-cooled plate has internal micro-channels supports the idea that the cooling circuit can induce mechanical vibrations and noise. This effect could be significantly reduced by replacing the water cooling of the pump diode by a thermo-electrical cooler.

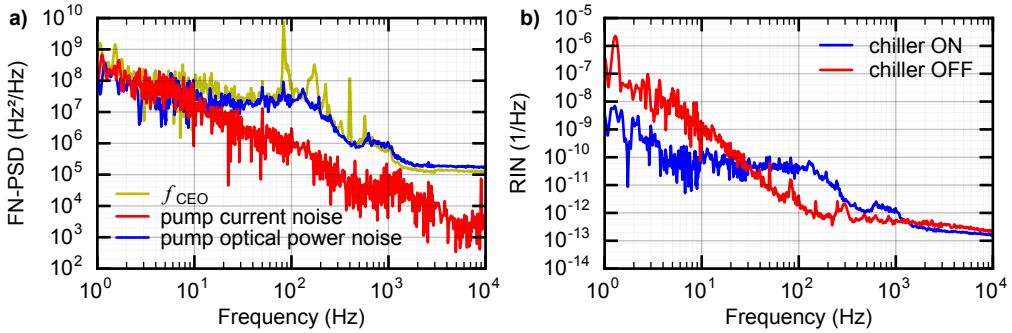

Fig. 9. a) FN-PSD measured for the free-running f_{CEO} (yellow) compared with the contributions of the current noise of the pump diode driver (red) and of the pump RIN (blue). The last two curves were obtained by converting the measured current noise and RIN into an equivalent frequency noise of the CEO by taking into account the slope efficiency of the pump diode and its pump-power-to-CEO-frequency transfer function. The water cooling chiller was in operation in this measurement. b) Comparison of the RIN of the pump diode measured with the water cooling chiller on (blue) and off (red).

5.3 Frequency stability

Whereas the frequency noise analysis presented above allows for the characterization of high-frequency noise components, a time-domain analysis reveals useful information about the long-term behavior of a frequency comb. For this purpose, we simultaneously recorded the time series of f_{rep} and f_{CEO} using a multi-channel Π-type frequency counter without dead-time (FXM-50 from K-K Messtechnik) with 1-s gate time. The 8th harmonic of f_{rep}, which was mixed down to a frequency of ~25 MHz in the measurement range of the counter, has been used in this measurement. This allowed us to ensure that the recorded frequency was not

Optics EXPRESS

limited by the 1-mHz counter resolution (which corresponds to a relative frequency resolution of 10^{-12} with respect to a 1-GHz signal).

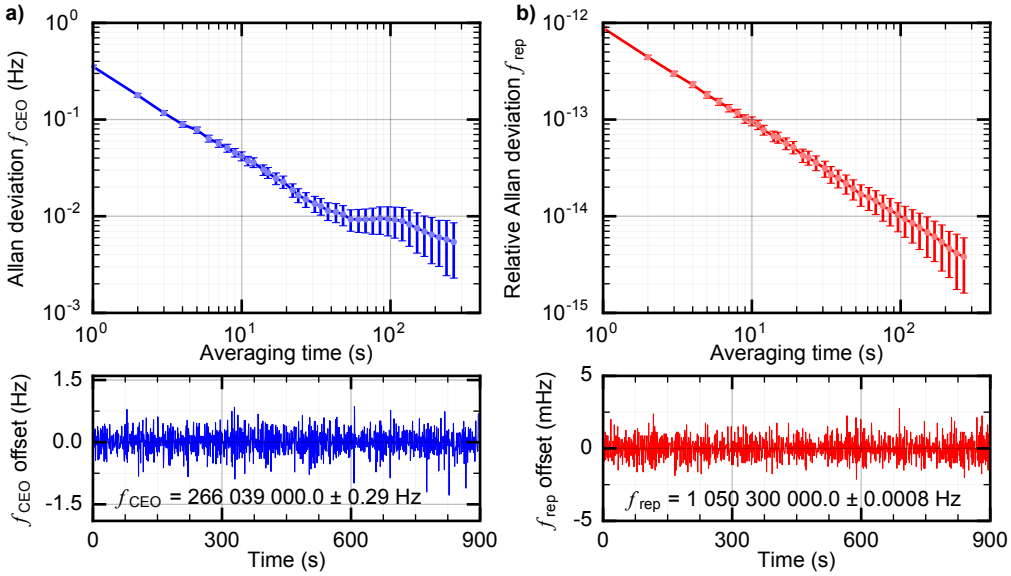

Fig. 10. Frequency stability of the fully-stabilized GHz comb: overlapped Allan deviation of f_{CEO} (a) and relative (overlapped) Allan deviation of f_{rep} (b) calculated from the recorded time series displayed in the bottom of the figure. The mean values and standard deviations of f_{CEO} and f_{rep} are also indicated on the plots.

Figure 10 shows a time series of 900 s simultaneously recorded for f_{rep} and f_{CEO} with the frequency counter and the corresponding calculated overlapped Allan deviation [37]. The relative frequency stability of f_{rep} in the range of 10^{-12} at 1-s averaging time is limited by the reference synthesizer used in the stabilization loop. The sub-Hz Allan deviation observed for f_{CEO} at an integration time of 1 s contributes at the level of 10^{-15} only to the relative frequency instability of an optical comb line at 1 µm (≈300 THz), which is negligible in comparison to the frequency instability arising from the repetition rate. Even if the comb was locked to an ultra-stable optical reference, the contribution of the CEO frequency instability to an optical comb line would not be dominant.

5.4 Characterization of an optical comb mode

Furthermore, we investigated the noise properties of an individual line of the fully-stabilized comb by implementing a heterodyne beat with a narrow-linewidth CW laser. Due to the lack of a suitable low-noise laser in the emission spectrum of our GHz comb, we developed a dedicated experimental setup to measure the noise of a comb line in comparison to an ultra-stable laser at 1557 nm (see bottom part of Fig. 1 and the Appendix for more details). This laser was stabilized to an ultra-low thermal expansion (ULE) optical cavity by the Pound-Drever-Hall locking technique, enabling a linewidth at the Hz level to be achieved. To link this laser to the GHz comb, a fully-stabilized Er:fiber frequency comb (FC1500 from Menlo Systems) with 250-MHz repetition rate and centered at 1.55 µm was used as a transfer oscillator. For this purpose, an additional SC spectrum extending down to the 1-µm range was generated from the modelocked Er:fiber oscillator using a highly non-linear fiber.

The FN-PSD of the virtual beat $f_{\text{virt. beat 2}}$ between one line of the GHz comb at 1030 nm and the ultra-stable laser at 1557 nm has been measured with the phase noise analyzer. Due to the negligible contribution of the ultra-stable laser (Hz level linewidth), this noise directly represents the noise of a comb line around 1030 nm, i.e. $\nu_N = N \cdot f_{rep} + f_{CEO}$ with $N \approx 276'600$.

Optics EXPRESS

To assess the noise contribution of $N{\cdot}f_{rep}$ for comparison, without limitation by the instrumental noise floor occurring when directly measuring f_{rep} in the RF domain, we produced a CEO-free virtual beat $f_{virt.beat\ 2}^{CEO\text{-}free}$ by mixing the virtual beat $f_{virt.\ beat\ 2}$ between the comb mode and the CW laser with the frequency-doubled CEO beat to remove its noise contribution (see details in Appendix). Figure 11(a) shows a comparison of the noise spectrum measured directly at the fundamental repetition rate f_{rep} and up-scaled to the optical frequency $N{\cdot}f_{rep}$ on one side, and obtained from the CEO-free virtual beat signal on the other side. The two curves overlap in the low frequency range up to ~10 kHz (they also coincide with the reference synthesizer below 100 Hz), and the optical measurement overcomes the noise floor limitation of the RF measurement occurring at frequencies higher than 10 kHz (corresponding to a white phase noise of −139 dBc/Hz).

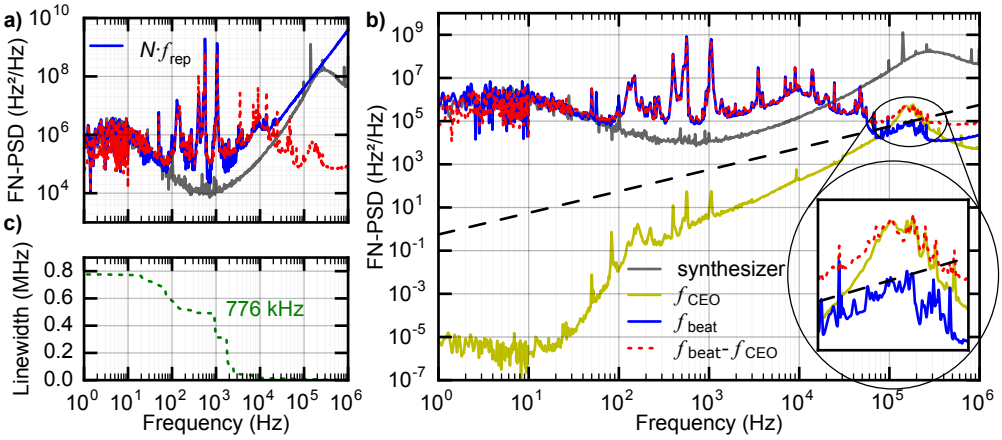

Fig. 11. a) Comparison of the FN-PSD of the repetition rate assessed from the direct measurement of f_{rep} in the RF domain (solid blue curve) and from the optical CEO-free virtual beat (dashed red curve), with a mode number $N \approx 276'600$, and of the reference synthesizer up-scaled by N^2 (gray). b) FN-PSD of an optical mode of the fully-stabilized GHz comb (blue), and comparison with the individual contribution of f_{CEO} (yellow), $N{\cdot}f_{rep}$ (red dashed) and of the reference synthesizer up-scaled by N^2 (gray). The inset shows a zoom in the frequency range of the CEO servo bump, where the noise of the optical comb line is lower than the individual contributions of f_{rep} and f_{CEO}. c) FWHM linewidth of the optical comb line calculated from the FN-PSD as a function of the low cut-off frequency (inverse of the observation time).

In Fig. 11(b), the noise spectrum of the optical line is compared to the individual contributions of $N{\cdot}f_{rep}$ and f_{CEO}. At low frequencies (1 to 100 Hz), the noise of the optical line coincides with the noise of the reference synthesizer, up-scaled by the factor N^2. In the frequency range of 100 Hz to 100 kHz, the noise of the optical line results from the excess noise of f_{rep}, whereas f_{CEO} has a negligible contribution. Furthermore, the FN-PSD of f_{CEO} is much lower than the β-separation line in this frequency range, indicating that it does not contribute to the linewidth of the optical comb line [35]. In the frequency range around 150 kHz, where the CEO servo bump is located, this is no longer the case and the CEO noise may contribute to the optical linewidth. In this frequency range [see inset of Fig. 11(b)], the FN-PSD of $N{\cdot}f_{rep}$ is very similar to the CEO noise, both in shape and amplitude (the two spectra overlap). However, the optical comb line has a noise lower than each of these individual contributions and lies underneath the β-separation line. The reason is that the noise in this spectral band mainly arises from the CEO servo-bump, which couples to the repetition rate as this degree of freedom of the comb is also affected by a modulation of the pump power, but with an opposite phase (anti-correlation). This anti-correlation combined with the similar amplitude of the noise of f_{rep} and f_{CEO} leads to a partial noise cancelation in the optical comb line $\nu_N = N{\cdot}f_{rep} + f_{CEO}$. A similar coupling of the CEO servo-bump in the frequency noise spectrum of f_{rep} and its partial compensation in the noise of an optical mode have been

Optics EXPRESS

previously observed in a fiber laser [36]. As a result, the servo-bump of f_{CEO} does not contribute to the optical linewidth of the comb mode, despite the fact that its integrated phase noise is not as low as in the first stabilization configuration of Fig. 7. From the measured FN-PSD of the comb line, its linewidth was calculated using the approximation of the β-separation line [35] and is displayed in Fig. 11(c) as a function of the low cut-off frequency of the FN-PSD (inverse of the observation time). An optical linewidth (full width at half maximum, FWHM) of ~800 kHz is obtained at 1-s observation time.

6. Conclusion

We have demonstrated the first self-referenced fully-stabilized GHz frequency comb from a DPSSL and have presented a detailed characterization of its noise and frequency stability properties. Frequency combs with GHz repetition rates offer several benefits over standard fiber-based combs that typically operate at 50-250 MHz only. A GHz repetition rate provides a higher power per mode (at constant average power), an easier access to individual comb lines, and an easier filtering of the beat-note with a continuous wave laser. So far, self-referenced fully-stabilized GHz frequency combs have been demonstrated only from Ti:Sapphire lasers. In comparison, DPSSL combs have the advantage of a simpler and cost-efficient diode pumping scheme, which enables direct high-bandwidth pump power modulation for CEO stabilization. In contrast, Ti:Sapphire combs have for a long time required an external acousto-optic modulator. Although a new green pump laser enabling direct and fast modulation was recently introduced in a commercial 1-GHz Ti:Sapphire comb [38], this pumping scheme is not as simple and cost-effective as the direct diode pumping of our Yb:CALGO laser. Furthermore, the fully-stabilized Yb:CALGO DPSSL reported here operates in the 1-µm wavelength range where low-noise narrow-linewidth continuous-wave lasers are easily available, opening attractive perspectives for future comb stabilization to an optical reference, instead of an RF reference as used in the results reported here.

The performed noise investigation of our GHz DPSSL comb included its two independent degrees of freedom, i.e., the repetition rate f_{rep} and the CEO frequency f_{CEO}, and additionally also an optical line at 1030 nm. This characterization was performed using a virtual heterodyne beat with an ultra-narrow linewidth CW laser at 1557 nm implemented with an auxiliary CW laser at 1030 nm and an Er:fiber comb used as a transfer oscillator.

The Yb:CALGO DPSSL with a repetition rate of 1.05 GHz was pumped with a commercial laser diode array wavelength-stabilized at 980 nm with a VHG. The self-starting SESAM-modelocked laser delivers an average output power of 2.1 W in 96-fs pulses. These properties were fully sufficient to generate a coherent octave-spanning SC spectrum for CEO self-referencing in a PCF directly from one of the two output beams of the oscillator, without any external amplification or pulse compression. The detected CEO beat with an SNR of 40 dB (in a 10-kHz RBW) and a free-running FWHM linewidth of ~500 kHz (over an observation time of ~1 s) was phase-locked with a bandwidth of ~150 kHz to an external frequency reference by feedback to the current of the pump diode using home-built fast modulation electronics. A tight lock of f_{CEO} was obtained with a residual integrated phase noise of 680 mrad [1 Hz - 1 MHz] in optimized stabilization conditions, corresponding to a fraction of more than 60% of the CEO power contained in the coherent peak.

The GHz repetition rate was phase-locked to a synthesizer referenced to an H-maser using a standard scheme of feedback to an intra-cavity PZT, resulting in an integrated timing jitter of 249 fs [10 Hz - 1 MHz]. This stabilization slightly affected the lock of f_{CEO} as a result of some cross-coupling effects, increasing the CEO integrated phase noise to 1.34 rad for an optimized lock of f_{rep}, but without any detrimental effect on the noise of an optical line. Our analysis showed the respective contribution of f_{rep} and f_{CEO} to the optical line, from which a linewidth in the range of 800 kHz was assessed, dominated by the residual noise of the repetition rate. The long-term relative frequency stability of the comb was also measured, limited at the level of 10^{-12} at 1-s averaging time by the reference synthesizer used in the

Optics EXPRESS

repetition rate stabilization, whereas the frequency instability of the locked CEO beat contributed only at the level of 10^{-15}/s.

Further improvements of the pump diode RIN and thus also of the general comb noise performance are expected by replacing the current water cooling circuit by Peltier coolers. In addition mechanical isolation of the laser cavity should reduce the influence of the mechanical noise that currently has a dominant effect on the noise of the repetition rate. Finally, a stabilization of the comb with a larger bandwidth will be investigated with the use of an opto-optical modulation of the intra-cavity SESAM [39], which has recently led to preliminary results in this laser [40].

Appendix (details of the comb line noise measurement)

We explain here how an optical line of the GHz comb at 1030 nm has been characterized with respect to an ultra-stable laser at 1557 nm. A first virtual beat $f_{\text{virt.beat 1}} = \nu_{1030}^{\text{GHz}} - \nu_{1030}^{\text{Er}}$ between one line of the SC spectrum generated from the Er:fiber comb (ν_{1030}^{Er}) and of the GHz comb (ν_{1030}^{GHz}) was detected at 1030 nm by combining (mixing) the beat signals between each comb and a distributed feedback (DFB) laser (Eagleyard DFB-1030-00100-BFW01-0002). The DFB laser was too noisy to enable a direct characterization of the GHz comb line and its noise cancelled out in the virtual beat as it was common to the two signals. The beat signal between the GHz comb and the DFB laser was realized after propagating the output of the Yb:CALGO oscillator in a few meters of singlemode fiber in order to slightly broaden its spectrum to reach the DFB laser wavelength of 1030 nm. As the noise spectrum of the virtual beat $f_{\text{virt.beat 1}}$ between the two combs was partially limited in some spectral regions by the Er:fiber comb, an additional virtual beat $f_{\text{virt.beat 2}}$ was realized between this signal and the 1557-nm ultra-stable laser, using the Er:fiber comb as a transfer oscillator. This was implemented by beating the Er:fiber comb, optically band-pass filtered at 1557 nm, with the cavity-stabilized narrow-linewidth laser, and by mixing this signal with the first virtual beat $f_{\text{virt.beat 1}}$. As these two beat signals contained a different noise contribution of the Er:fiber comb (due to the different upscaling factor of the dominant repetition rate noise by the mode number N_{1030}^{Er} or N_{1557}^{Er} involved in the two beats), they had to be scaled by a factor $N_{1557}^{\text{Er}} : N_{1030}^{\text{Er}} \approx 0.66$ prior to be mixed following the principle of the transfer oscillator [41]. We did not implement here a perfect transfer oscillator with the exact factor $N_{1557}^{\text{Er}} : N_{1030}^{\text{Er}}$, but we approximated it by a value of 2:3 that was fully sufficient to suppress the noise contribution of the Er:fiber comb in the considered measurement. Therefore, the first virtual beat $f_{\text{virt.beat 1}}$ and the heterodyne beat at 1557 nm have been frequency doubled and tripled, respectively, before being filtered, amplified, and mixed together. The CEO beat $f_{\text{CEO}}^{\text{Er}}$ of the Er:fiber comb has not been removed from this virtual beat, but we have checked that its contribution to the measured noise spectrum was negligible. Finally, the virtual beat between the GHz comb line at 1030 nm (ν_{1030}^{GHz}) and the ultra-stable laser at 1557 nm (ν_{1557}) is given by:

$$f_{\text{virt.beat 2}} = \left|2\left(\nu_{1030}^{\text{GHz}} - N_{1030}^{\text{Er}} f_{\text{rep}}^{\text{Er}} - f_{\text{CEO}}^{\text{Er}}\right) - 3\left(\nu_{1557} - N_{1557}^{\text{Er}} f_{\text{rep}}^{\text{Er}} - f_{\text{CEO}}^{\text{Er}}\right)\right| \approx \left|2\nu_{1030}^{\text{GHz}} - 3\nu_{1557} + f_{\text{CEO}}^{\text{Er}}\right|$$

This virtual beat, in which the noise of the Er:fiber comb was cancelled to a large extent, was finally analyzed. It contained two times the noise of the investigated line ν_{1030}^{GHz} of the GHz comb. A CEO-free virtual beat that contained only the noise contribution of $N \cdot f_{\text{rep}}$ was finally obtained by mixing the virtual beat with the frequency-doubled CEO beat of the GHz comb to cancel its noise contribution:

Optics EXPRESS

$$f_{\text{virt.beat 2}}^{\text{CEO-free}} \approx \left| 2\nu_{1030}^{\text{GHz}} - 3\nu_{1557} + f_{\text{CEO}}^{\text{Er}} \right| - 2f_{\text{CEO}} \approx 2N \cdot f_{\text{rep}} - 3\nu_{1557} + f_{\text{CEO}}^{\text{Er}}$$

Funding

This work was supported by the Swiss Commission for Technology and Innovation (CTI) under the contract No. 17137.1 PFMN-NM. The ultra-stable laser and experimental scheme used to characterize the comb optical line were developed in the frame of the Marie-Curie International Training Network project FACT (Future Atomic Clock Technologies) of the European Union's Seventh Framework Programme for research, technological development and demonstration, under the grant agreement No PITN-GA-2013-607493.